A financial hyperchaotic system with coexisting attractors: dynamic investigation, entropy analysis, control and synchronization

Hadi Jahanshahi[1], Amin Yousefpour[2], Zhouchao Wei[3], Raúl Alcaraz[4], Stelios Bekiros[5,6]

[1]Department of Aerospace Engineering, Faculty of New Sciences and Technologies, University of Tehran, Tehran, 14395 -1561, Iran; hadi_jahanshahi@ut.ac.ir

[2]School of Mechanical Engineering, College of Engineering, University of Tehran, Tehran, 14399–57131, Iran; amin.yusefpour@ut.ac.ir

[3]School of Mathematics and Physics, China University of Geosciences, Wuhan, 430074, P. R. China; weizhouchao@163.com

[4]Research Group in Electronic, Biomedical and Telecommunication Engineering, University of Castilla-La Mancha (UCLM), 16071 Cuenca, Spain; raul.alcaraz@uclm.es

[5]European University Institute, Department of Economics, Via delle Fontanelle, 18, I-50014, Florence, Italy; stelios.bekiros@eui.eu

[6]Rimini Centre for Economic Analysis (RCEA), LH3079, Wilfrid Laurier University, 75 University Ave W., ON, N2L3C5, Waterloo, Canada

Abstract

This paper is concerned with dynamic and entropy analyses of a hyperchaotic financial system, as well as with its hyperchaos suppression and synchronization. The dynamic behaviour of the system is analyzed for several parameters and initial conditions making use of bifurcation diagrams, Lyapunov exponents and phase portraits. Moreover, entropy from resulting time series is also characterized by estimating ordinal pattern distributions. These analyses have been able to determine and locate accurately chaotic and periodic attractors in the system, thus enabling successful design of its control. In general, financial systems are not always completely synchronized; therefore, some robust synchronization technique should be considered. This study proposes a novel fuzzy disturbance-observer based integral terminal sliding mode control method for the hyperchaotic financial system. The presented control technique guarantees robustness against uncertainties, external disturbances and control input saturation. Fuzzy rules are employed to adaptively tune the gains of the proposed control scheme. Also, the fuzzy inference engine avoids the chattering problem in the system response. Simulation results illustrate the efficient performance of the proposed control technique in presence of dynamic uncertainties, external disturbances and control input saturation.

Keyword: hyperchaotic financial system; dynamic analysis, entropy analysis, fuzzy disturbance-observer based integral terminal sliding mode control method; dynamic uncertainties; external disturbances; control input saturation.

1. Introduction

The introduction of the Rössler system led to the formation of a new platform in the nonlinear system researches, called hyperchaos [1]. The hyperchaotic systems have been widely studied due to their interesting properties, such as high efficiency, high security, and high capacity. Nowadays, these systems have been used in a variety of fields, including cryptography, imitation of the neural system, and image encryption. After the Rössler system, the hyperchaotic Chen system [2], Lu system [3], and hyperchaotic Nikolov system [4] have been introduced. The hyperchaos phenomena in financial systems may turn into financial crises, such as bogging down the market and taking it out control [5, 6]. In addition, this phenomenon could threaten investment safety [7]. Over the past few decades, several high-dimensional economical models, such as the Behrens-Feichtinger model [8], the Cournot-Puu system [9], and other four-dimensional hyperchaotic financial systems [10, 11], have been introduced.

During the past several decades, many control schemes, such as the feedback linearization [12, 13], backstepping method [14, 15], intelligent control [16, 17], adaptive control [18, 19], and sliding mode control (SMC) [20, 21], have been applied to control nonlinear systems. In recent years, several studies have also introduced control methods to maintain specific characteristics and behaviours in hyperchaotic finance systems. Hołyst and Urbanowicz have proposed a time-delayed feedback technique for the control of chaotic behaviour of an economic model [8]. Yao et al. have developed a straight-line stabilization technique to achieve chaos control in economic models [22]. Vargas et al. have presented an adaptive control technique for a hyperchaotic financial system [23]. Jajarmi et al. have proposed an optimal controller with Pontryagin's maximum principle to stabilize the hyperchaos behaviour of a finance system [24]. Also, some other studies have suggested sliding mode techniques to control chaos in economical systems [25, 26].

Among the stated techniques, SMC has gained significant attention in various applications due to its interesting properties, such as guaranteed stability, computational simplicity and robustness against uncertainties [27]. Nevertheless, SMC may not give an assurance that the closed-loop system converges to the desired trajectory in finite time. Hence, terminal SMC (TSMC) has been proposed to guaranty finite-time convergence of the closed-loop system [28, 29]. On the other hand, integral SMC (ISMC) and integral TMSC (ITSMC) have been developed to improve robustness in the performance of SMC and TSMC [30, 31]. Actually, by adding an integral term to conventional SMC and TSMC, the reaching phase of the sliding surface is eliminated, and states of the system start moving on the sliding surface right from any initial conditions. Therefore, the robustness of the control scheme improves in the entire state space [32, 33]. These capabilities explain that ISMC and ITSMC have received much attention and have been proposed for uncertain nonlinear systems [31, 34].

Most of financial systems in practical applications possess uncertain nonlinear dynamics in presence of control input limitation and external disturbances [35]. This chaotic response can potentially increase fluctuations in economic systems [24]. On the other hand, input saturation is a non-smooth nonlinearity which should be considered in the control design for economic systems. To address these problems, further study on the control methods is required to achieve higher performance in controlling nonlinear systems.

In this paper, we implement the four-dimensional financial hyperchaotic system proposed by Yu et. al. [11] and its dynamical behaviour is featured through bifurcation diagrams, phase portraits, and Lyapunov exponents diagrams. Entropy is also computed by estimating ordinal pattern distributions from the resulting time series. When the same parameters are used, these analyses show different dynamics as a function of the initial conditions, thus getting coexisting attractors of the system and enabling successful design of its control. In fact, this study also introduces a novel control scheme for chaos suppression and synchronization of the system combining fuzzy logic with fast disturbance observer and ITSMC. The proposed control technique guarantees robustness with regard to external disturbances and reduces the chattering for the MIMO uncertain nonlinear system in presence of control input saturation, such as extensive simulation results exhibit.

The rest of the paper is organized as follows. Firstly, nonlinear dynamics of the four-dimensional financial hyperchaotic system are studied in Section 2. In Section 3, a time series-based entropy analysis using ordinal pattern estimations is implemented. In Section 4, the combination of fast disturbance observer, ITSMC and fuzzy logic is proposed. Also, based on Lyapunov stability theorem, Finite time stability, the convergence of the closed-loop system is proved. In Section 5, the hyperchaotic finance system is considered in presence of the external disturbance, dynamic uncertainty and limitation control input numerical. Numerical simulations illustrating the performance and effectiveness of the proposed controller for chaos suppression and synchronization are also shown in this section. Moreover, the presented controller is compared with the disturbance-observer-based SMC, which is developed by Chen and Chen [36]. Finally, concluding remarks are given in Section 6.

2. Financial hyperchaotic system

The four-dimensional financial hyperchaotic system, which is defined by two positive Lyapunov exponents, can be defined as follows [11]:

$$\begin{aligned} \dot{x} &= z + (y - a)x + u \\ \dot{y} &= 1 - by - x^2 \\ \dot{z} &= -x - cz \\ \dot{u} &= -dxy - ku \end{aligned} \tag{1}$$

Its basic dynamics can be summarized in the following Lyapunov exponents and bifurcation diagrams for b in $[0.1,0.5]$, when $a = 0.9$, $c = 1.5$, $d = 0.2$, and $k = 0.17$. Figure 1 shows the Lyapunov exponents for initial values $(0.1,0.2,0.6,-0.3)$ and the corresponding bifurcation diagram of the state variable x in Figure 2. Figure 3 shows the corresponding bifurcation diagram of the state variable x when the initial values are $(0,2,0.1,-0.5)$. As can be seen, although we have chosen the same parameter conditions, we can still get different bifurcation diagrams for different initial values. Therefore, we can obtain the coexisting attractors displayed in Figure 4.

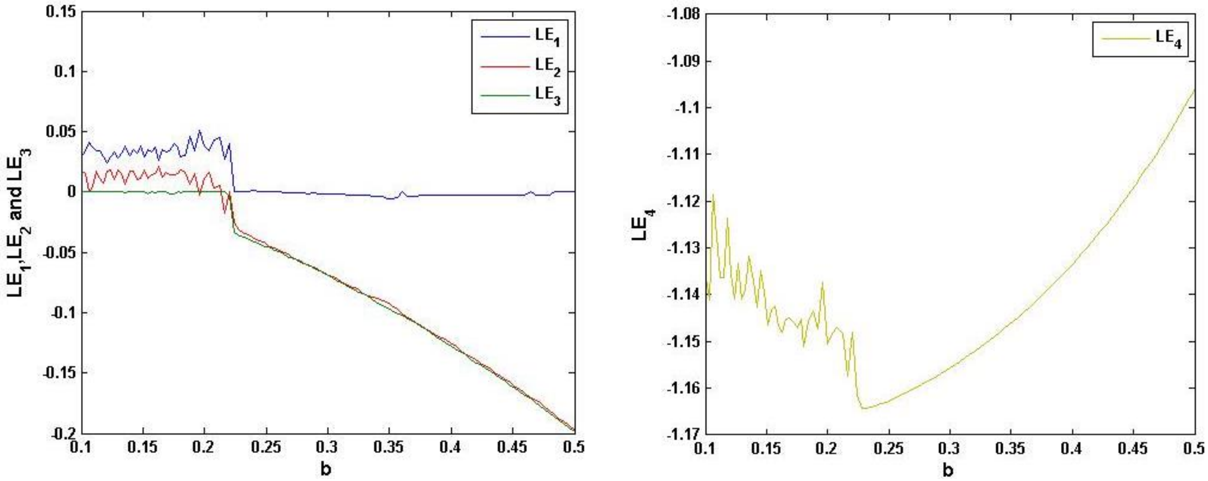

Figure 1: Lyapunov exponents for $a = 0.9$, $c = 1.5$, $d = 0.2$, $k = 0.17$ and b in [0.1,0.5] and initial values $(0.1,0.2,0.6,-0.3)$.

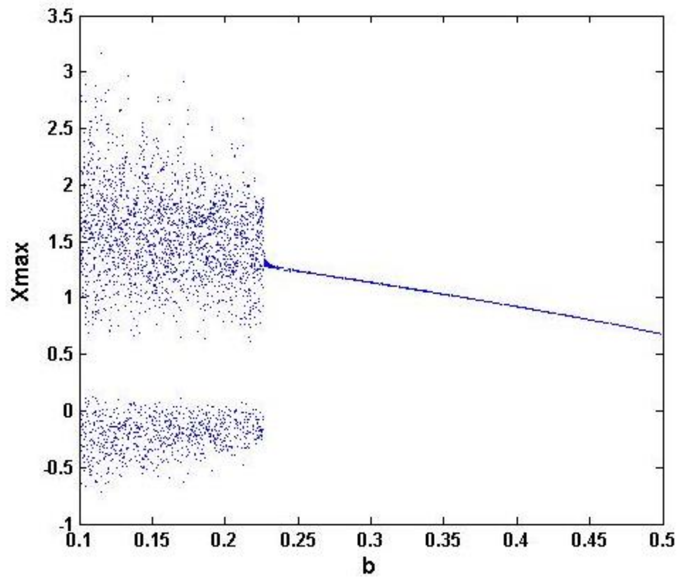

Figure 2: Bifurcation diagram for $a = 0.9$, $c = 1.5$, $d = 0.2$, $k = 0.17$ and b in [0.1,0.5] and initial values $(0.1,0.2,0.6,-0.3)$

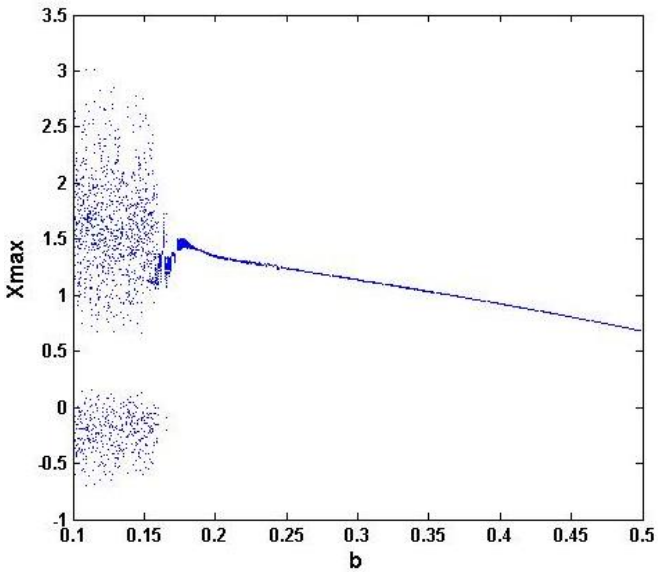

Figure 3: Bifurcation diagram for $a = 0.9$, $c = 1.5$, $d = 0.2$, $k = 0.17$ and b in $[0.1, 0.5]$ and initial values $(0,2,0.1,-0.5)$.

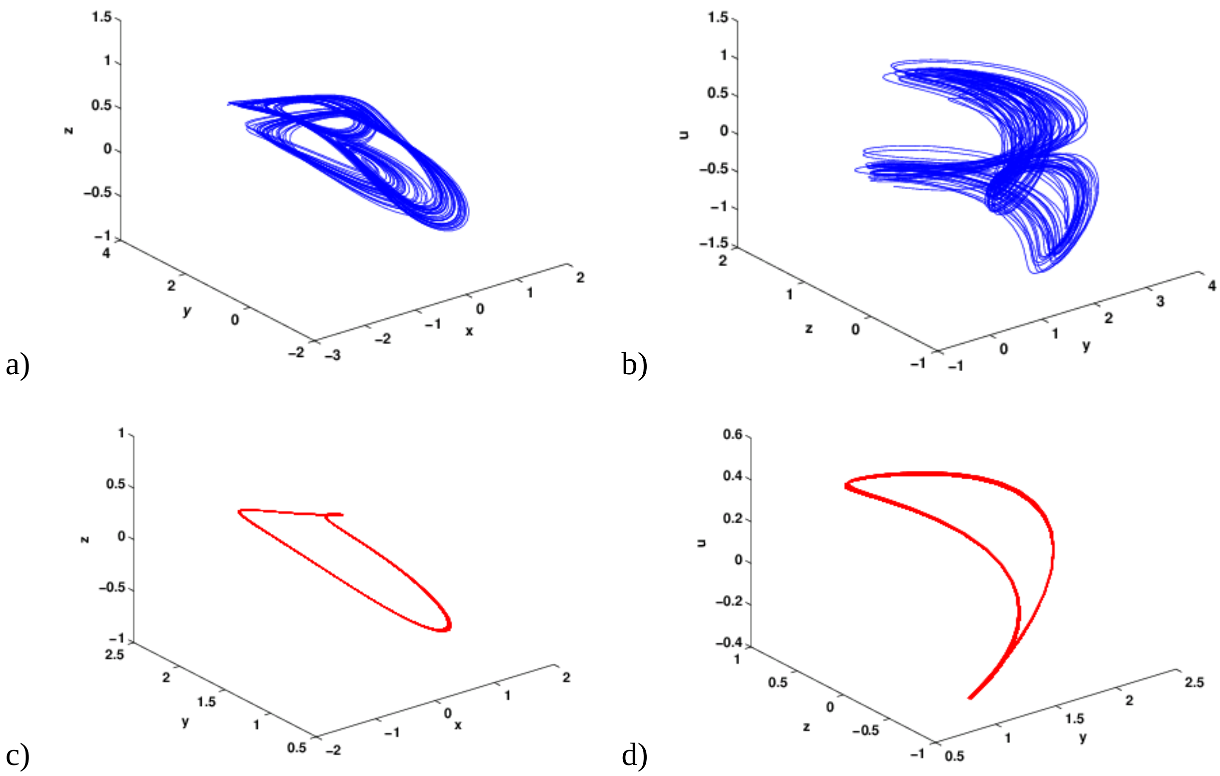

Figure 4: Coexisting attractors for $a = 0.9$, $b = 0.2$, $c = 1.5$, $d = 0.2$, $k = 0.17$. (a) and (b): hyperchaos with initial values $(0.1,0.2,0.6,-0.3)$; (c) and (d): periodic orbit with initial values $(0,2,0.1,-0.5)$.

3. Entropy analysis

Beyond the analysis of bifurcation diagrams and Lyapunov exponents, entropy is often studied for a broader understanding of the dynamical characteristics of systems [37]. In fact, entropy of a system is characterized by unpredictability of its dynamics, so that more complex systems are less predictable [38]. To estimate this information, some theoretical measures, including the well-known Kolmogorov-Sinai entropy, have been proposed. However, they present some difficulties to compute entropy from finite time series [39]. To address this limitation, several empirical measures have been developed, such as approximate entropy [39] or sample entropy [40], but their theoretical foundation is lost [41]. Contrarily, the theoretical basis as well as its relationship with Kolmogorov-Sinai entropy have been clearly established for permutation entropy (PerEn) [42]. This index is based on an ordinal pattern analysis and can be applied to any kind of data set. Moreover, because PerEn is a conceptually simple, computationally fast, and noise-robust measure, it has been used to characterize a wide variety of real-world time series [43].

From a mathematical point of view, given a time series of N samples in length, i.e., $x(n) = \{x(1), x(2), \dots, x(N)\}$, the first step to compute PerEn is to form $N - m + 1$ vectors of size m samples, such that $X_m(i) = \{x(i), x(i+1), \dots, x(i+m-1)\}$, for $1 \le i \le N - m + 1$. Next, an ordinal pattern is associated to each vector $X_m(i)$, which is defined as the permutation $\kappa_i = \{r_0, r_1, \dots, r_{m-1}\}$ of $\{0,1, \dots, m-1\}$ that fulfills $x(i + r_0) \le x(i + r_1) \le \cdots \le x(i + r_{m-2}) \le x(i + r_{m-1})$. Thus, $m!$ different ordinal patterns, referred to as π_k, can be obtained from vectors X_m. The occurrence probability of each pattern π_k can then be estimated by its relative frequency, such that

$$p(\pi_k) = \frac{\sum_{i=1}^{N-m+1} \delta(\pi_k, \kappa_i)}{N - m + 1} \qquad (2)$$

where $\delta(u, v)$ is the Kronecker delta function modified to work with patterns, i.e.

$$\delta(u,v) = \begin{cases} 1 & \text{if } u(i) = v(i), \text{for every } i = 1,2,\dots,m; \text{and} \\ 0 & \text{for otherwise.} \end{cases} \quad (3)$$

Finally, entropy is estimated by computing Shannon entropy from the probability distribution for all the symbols, such that

$$\text{PerEn}(m) = -\frac{1}{\ln(m!)}\sum_{k=1}^{m!} p(\pi_k)\ln(p(\pi_k)) \quad (4)$$

It should be noted that PerEn is normalized by its highest value, i.e. $\ln(m!)$, thus ranging between 0 and 1 [44]. Whereas a completely predicable time series defined by a single pattern is featured by a value of 0, the largest entropy of 1 is obtained when all symbols π_k exhibit the same occurrence probability. Nonetheless, right selection of m plays a key role to obtain robust PerEn estimates. To this respect, higher values of m allow to consider a greater number of different patterns, thus usually providing more reliable entropy estimates. However, the higher the value of m, the higher the computational load, and a trade-off between both aspects has been strongly suggested [45]. Thus, values of m between 3 and 7 have only been previously recommended by several authors [42-44].

After several experiments with these values of m, no significant differences were noticed in PerEn evolution as a function of parameter b. Thus, Figure 5 shows PerEn values computed from the time series $x(n)$ for $m = 7$ and the two initial conditions previously considered, i.e. $(0.1, 0.2, 0.6, -0.3)$ and $(0, 2, 0.1, -0.5)$. As can be observed, for both cases entropy values agree with bifurcation diagrams presented in Figures 2 and 3. Precisely, PerEn exhibits high values when the system is in a chaotic state and, on the contrary, low estimates when it is in a stable state.

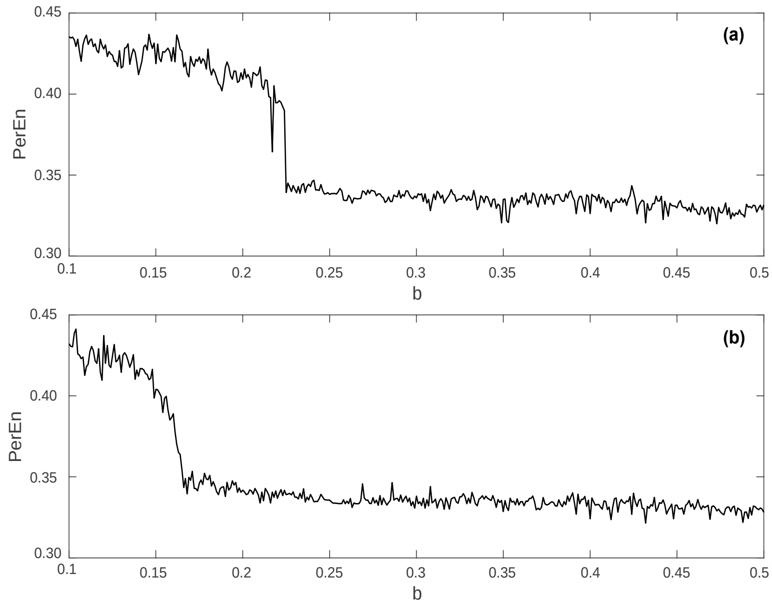

Figure 5: PerEn evolution as a function of parameter b for initial conditions of (a) $(0.1,0.2,0.6,-0.3)$ and (b) $(0,2,0.1,-0.5)$.

4. Controller design

Consider the following MIMO nonlinear relative-degree-one systems with dynamic uncertainties and external disturbance:

$$\dot{x}(t) = f(x) + \Delta f(x) + \big(g(x) + \Delta g(x)\big)u_c + d_0(t) \tag{5}$$

where $x = [\, x_1 , x_2 , \dots , x_n \,]^T$ denotes state vector, $f(x)$ is nonlinear functions representing system dynamics and g is a $n \times n$ nonlinear matrix. Moreover, Δf and Δg are the nonlinear functions indicating the system uncertainties. The vector, $d_0 = \left[\, d_{0\_1} , d_{0\_2} , \dots , d_{0\_n} \,\right]^T$ and $u_c = [\, u_{c1} , u_{c2} , \dots , u_{cn} \,]^T$ denote the external disturbance and control input, respectively. Considering the uncertain terms of the system and the external disturbance (d_0) as a single disturbance term $d\,(t\,)$, the dynamic equation of the system can be written as

$$\dot{x}(t) = f(x) + g(x)u_c + d(t) \tag{6-a}$$

$$d(t) = \Delta f(q) + \Delta g(q) u_c + d_0(t)) \tag{6-b}$$

The lemma 1 and 2 are used in order to propose the disturbance-observer-based ITSMC for the uncertain MIMO nonlinear relative-degree-one systems (5).

Lemma 1. Let continuous positive definite function $V(t)$, which fulfills the following inequality [46]:

$$\dot{V}(t) + \vartheta V(t) + \xi V^{\chi} \leq 0, \quad \forall t > t_0 \tag{7}$$

where $0 < \chi < 1$, and $\vartheta > \xi > 0$. As a result, the function $V(t)$ converges to the equilibrium point in the finite time t_s,

$$t_s \leq t_0 + \frac{1}{\vartheta(1+\chi)} \ln \frac{\vartheta V^{1-\chi}(t_0) + \xi}{\xi} \tag{8}$$

Lemma 2. By considering triangle inequality: if $0 < n < 1$ and $a_\Delta > 0, \Delta = 1, 2, \dots, m$, then

$$\left(\sum_{\Delta=1}^{m} a_\Delta \right)^n \leq \sum_{\Delta=1}^{m} a_\Delta^n \tag{9}$$

4.1. Fast disturbance observer in the presence of control input saturation

However, in real systems, where the maximum and minimum amount of the control input has certain restrictions, control input saturation as a non-smooth nonlinearity may occur in many practical systems. Therefore, in this study, the unknown input saturation has been considered. By applying the input saturation constraints, the control input u which applied to the system is as follows

$$u_c = \begin{cases} u_{max} & if\ v > u_{max} \\ v & \\ u_{min} & if\ v < u_{min} \end{cases} \tag{10}$$

where u_{min} and u_{max} are the maximum and minimum bounds of control input saturation and v is the control input which will be obtained in the following with integral terminal sliding mode technique. Now, considering $\tilde{u}_c = u_c - v$ and replacing Eq. (10) into Eq. (6) yields

$$\begin{aligned} \dot{x}(t) &= f(x) + g(x)(v + \tilde{u}_c) + d \\ &= f(x) + g(x)v + g(x)\tilde{u}_c + d \\ &= f(x) + g(x)v + D \end{aligned} \tag{11}$$

where $D = g(x)\tilde{u}_c + d$ is a compound disturbance by applying control input saturation. To design a finite time disturbance observer, the following auxiliary variables is defined [47]:

$$s_d = z - x \tag{12}$$

in which variable z is given by

$$z = -k_d s_d - \beta sign(s_d) - \varepsilon {s_d}^{p_0/q_0} - |f(x)| sign(s_d) + g(x)v \tag{13}$$

where design parameters k_d and ε are positive and $\beta > \|D\|_1$, and symbol $\|.\|$ denotes 1-norm. Also, p_0 and q_0 are odd positive integers, which $p_0 < q_0$. The fast disturbance observer $\widehat{D}$ is given by

$$\widehat{D} = -k_d s_d - \beta sign(s_d) - \varepsilon {s_d}^{p_0/q_0} - |f(x)| sign(s_d) - f(x) \tag{14}$$

Considering Eqs. (12), (13), and (11) the following equation has been achieved

$$\dot{s_d} = \dot{z} - \dot{x}_n = -k_d s_d - \beta \text{sign}(s_d) - \varepsilon {s_d}^{p_0/q_0} - |f(x)| \text{sign}(s_d) - f(x) - D \tag{15}$$

According to Eqs. (11), (14), and (15), we have

$$\begin{aligned} \widetilde{D} = \widehat{D} - D &= -k_d s - \beta \text{sign}(s) - \varepsilon s^{\frac{p_0}{q_0}} - |f(x)| \text{sign}(s) - f(x) - D \\ &= -k s_d - \beta sign(s_d) - \varepsilon {s_d}^{\frac{p_0}{q_0}} - |f(x)| sign(s_d) - f(x) - \dot{x} + f(x) + g(x)v \\ &= -k s_d - \beta sign(s_d) - \varepsilon {s_d}^{\frac{p_0}{q_0}} - |f(x)| sign(s_d) + g(x)v - \dot{x} = \dot{z} - \dot{x} = \dot{s_d} \end{aligned} \tag{16}$$

Lemma 3 and Theorem 1 have been employed to prove the stability and tracking of the disturbance estimation in the finite time.

Theorem 1. For the MIMO uncertain nonlinear system (6), by applying disturbance estimator (12)-(15), the error of disturbance observer is convergent to zero, in the finite time.

Proof. assume the positive definite Lyapunov function candidate as

$$V_0 = \frac{1}{2} {s_d}^T s_d \tag{17}$$

The time derivative of the function V_0 is:

$$\begin{aligned} \dot{V}_0 &= {s_d}^T \dot{s_d} = {s_d}^T \left(-k_d s_d - \beta sign(s_d) - \varepsilon {s_d}^{\frac{p_0}{q_0}} - \|f(x)\|_1 sign(s_d) - f(x) - D\right) \\ &\le -k_d {s_d}^T s_d - \beta {s_d}^T \mathrm{sign}(s_d) - \varepsilon {s_d}^T {s_d}^{\frac{p_0}{q_0}} - \|f(x)\|_1 \; {s_d}^T sgn(s_d) - {s_d}^T f(x) - {s_d}^T D \\ &\le -k_d {s_d}^T s_d - \beta \|{s_d}^T\|_1 - \varepsilon {s_d}^T {s_d}^{\frac{p_0}{q_0}} - \|f(x)\|_1 \|{s_d}^T\|_1 - {s_d}^T f(x) + \|{s_d}^T\|_1 \|D\|_1 \\ &\le -k_d {s_d}^T s_d - \varepsilon {s_d}^T {s_d}^{\frac{p_0}{q_0}} \le -2kV_0 - 2^{(p_0+q_0)/2q_0} \varepsilon V_0^{(p_0+q_0)/2q_0} \end{aligned} \tag{18}$$

The last line of Eq. (18) has been obtained by Lemma 3.

Lemma 3.

$$\begin{aligned} &V_0 = \frac{1}{2} {s_d}^T s_d = \frac{1}{2}({s_d}_1^2 + {s_d}_2^2 + \cdots + {s_d}_n^2) \\ &V_0^{(p_0+q_0)/2q_0} = \left(\frac{1}{2}\left({s_d}_1^2 + {s_d}_2^2 + \cdots + {s_d}_n^2\right)\right)^{(p_0+q_0)/2q_0} \\ &\le \frac{1}{2^{(p_0+q_0)/2q_0}} \left({s_d}_1^{(p_0+q_0)/2q_0} + {s_d}_2^{(p_0+q_0)/2q_0} + \cdots + {s_d}_n^{(p_0+q_0)/2q_0}\right) \end{aligned} \tag{19}$$

Therefore, the following equation has been achieved

$$2^{(p_0+q_0)/2q_0} V_0^{(p_0+q_0)/2q_0} \le {s_d}_1^{(p_0+q_0)/q_0} + {s_d}_2^{(p_0+q_0)/q_0} + \cdots + {s_d}_n^{(p_0+q_0)/q_0} \tag{20}$$

As we know ${s_d}_1^{(p_0+q_0)/q_0} + {s_d}_2^{(p_0+q_0)/q_0} + \cdots + {s_d}_n^{(p_0+q_0)/q_0} = {s_d}^T {s_d}^{p_0/q_0}$, thus

$$2^{(p_0+q_0)/2q_0} V_0^{(p_0+q_0)/2q_0} \leq {s_d}^T {s_d}^{\frac{p0}{q_0}}$$
$$\xrightarrow{yields} -\varepsilon {s_d}^T {s_d}^{p0/q_0} \leq -\varepsilon 2^{(p_0+q_0)/2q_0} V_0^{(p_0+q_0)/2q_0} \tag{21}$$

According to Lemma 1,2 and 3 and Eq. (18) the proposed disturbance estimator satisfies the Lyapunov condition and the disturbance approximation error $\widetilde{D}$ converge to zero in the finite time.

Remark 1. According to Lemma1 the disturbance estimator which proposed for the MIMO nonlinear system converges to zero in finite time. The convergence time of the disturbance observer given by

$$t_{s\Delta} < t_{0\Delta} + \frac{q_0}{k(p_0 + 3q_0)} \ln\left(\frac{k s_{0\Delta}^{(q_0-p_0)/\,q_0} \; t_{0\Delta}}{\varepsilon} + 1\right) \qquad \Delta = 1,2,3\ldots,n \tag{22}$$

in which, $t_{s\Delta}$ and $t_{0\Delta}$ are convergence time of each element and initial time, respectively.

4.2. ITSMC

By utilizing the output of disturbance observer, the ITSMC is employed to achieve the control objective $\lim_{t\to\infty} x(t) = x_d(t)$ in the presence of dynamic uncertainty, external disturbance and control input saturation. The vector of tracking error of the system is given by

$$e(t) = [e_1(t), e_2(t), \ldots, e_n(t)]^T = x(t) - x_d(t) \tag{23}$$

To develop the integral terminal sliding mode tracking controller the following variable will define as [48]:

$$s_c(t) = e(t) + \alpha \int_0^t e^{p/q}(\tau) d\tau \quad \text{and} \quad s_c(0) = 0 \tag{24}$$

where parameters q and p are odd integers and $q > p > 0$. when $s_c(t) = 0$, Eq. (24) is equivalent to

$$e(t) = -\alpha \int_0^t e^{\frac{p}{q}}(\tau)d\tau \quad (25)$$

First-order differentiation of both side of Eq. (25) yields:

$$\dot{e}(t) = -\alpha e^{p/q} \quad (26)$$

Integrating of Eq (26), yields

$$\alpha \int_{T_i}^{T_f} d\tau = -\int_{e(T_i)}^{e(T_f)} \frac{1}{e^{p/q}} de \quad (27)$$

By solving Eq. (27), the convergence time of $s_c(t)$ is achieved as

$$T_f = T_i + \frac{e(T_i)^{1-p/q}}{\alpha^{1-p/q}(1-\frac{p}{q})} = \frac{e(T_i)^{1-p/q}}{\alpha^{1-p/q}(1-\frac{p}{q})} \quad (28)$$

The time derivative of the variable $s_c(t)$ along trajectories of dynamics (11) yields

$$\dot{s_c}(t) = \dot{e} + \alpha e^{\frac{p}{q}}(t) = f(x) + g(x)v + D(x) - \dot{y_d} + \alpha e^{\frac{p}{q}}(t) \quad (29)$$

By considering the fast disturbance observer, the integral terminal sliding surface can be defined as

$$s_t(t) = s_c(t) + s_d(t) \quad (30)$$

in which $s_d(t)$ is the auxiliary variable related to the disturbance observer which introduced in equation (12). The disturbance-observer-based ITSMC for the MIMO nonlinear uncertain system (11) in the presence of unknown non-symmetric input saturation is designed as

$$v = g^{-1}(x)\left(\dot{x}_d - f(x) - \left(K + \delta \left\|e^{\frac{p}{q}}(t)\right\| I\right) \text{sign}(s_t) - \widehat{D}\right) \quad (31)$$

where parameters K, δ, and α are positive which $\delta > \alpha$ and K is

$$K = dig([k_1, k_2, \ldots, K_n]) \quad (32)$$

Theorem 2. The states of the closed-loop system (5) are convergence to the desired value in the finite time by using the proposed control law (31).

Proof. Choose the positive-definite Lyapunov candidate functional as follow

$$V_0 = \frac{1}{2} s_t^T s_t \tag{33}$$

Taking the time derivative of the Lyapunov function candidate and using Eqs. (31) and (11) yields

$$\begin{aligned} \dot{V}_0 &= s_t^T \dot{s}_t = s_t^T \left(f(x) + g(x)u - \dot{x_d} + \alpha e^{\frac{p}{q}}(t) + \dot{s}_t \right) \\ &= s_t^T \left(f(x) + \left(\dot{x}_d - f(x) - \left(K + \delta \left\| e^{\frac{p}{q}}(t) \right\| I \right) \mathrm{sign}(s_t) - \widehat{D} \right) - \dot{x_d} + \alpha e^{\frac{p}{q}}(t) + \dot{s}_d \right) \\ &= s_t^T \left(-\left(K + \delta \left\| e^{\frac{p}{q}}(t) \right\| I \right) \mathrm{sign}(s_t) + D - \widehat{D} + \alpha e^{\frac{p}{q}}(t) + \dot{s}_d \right) \\ &= s_t^T \left(-\left(K + \delta \left\| e^{\frac{p}{q}}(t) \right\| I \right) \mathrm{sign}(s_t) + \widetilde{D} + \alpha e^{\frac{p}{q}}(t) + \dot{s}_d \right) \end{aligned} \tag{34}$$

Considering Eq (12) $\widetilde{D} = -\dot{s}_d$ yields

$$s_t^T \dot{s}_t = -s_t^T \left(K + \delta \left\| e^{\frac{p}{q}}(t) \right\| I \right) \mathrm{sign}(s_t) + s_t^T \alpha e^{\frac{p}{q}}(t) \tag{35}$$

where parameters K, δ and α are positive, and $\delta > \alpha$, hence

$$s_t^T \dot{s}_t \leq -(K) \| s_t \| \tag{36}$$

In conclusion, the designed control scheme satisfies the Lyapunov condition. Accordingly, it can be established that all state of the closed-loop system converges to the desired value in the finite time.

4.3 Fuzzy inference logic for disturbance-observer-based ITSM

To avoid the chattering phenomenon caused by the discontinuous function $sgn\,(.)$ and to increase the speed of converging to the desired value, the following fuzzy controller have been proposed. The fuzzy inference engine adaptively tunes the gains of the controller. This way, the fuzzy logic map the input variables $s_t, \dot{s}_t, s_d$, and $\dot{s}_d$ to the output variables F_{st}, F_{sd} K and k_d. Where the matrix

K and k_d are design parameter of controller and F_{st}, F_{sd} are substitutions of the $sign(\ s_t)$ and $sign(\ s_d)$. The fuzzy rules are chosen somehow satisfy the stability of the proposed control technique. According to stability conditions of the disturbance-observer-based ITSMC which described in Eq.(36), negativeness or positiveness of F_{st}, F_{sd} is taken from $sign\ (s_t)$ and $sign\ (s_d)$.

In the present study, the Mamdani fuzzy controller has been applied. Max operator is used for the aggregation of the rules. Moreover, Min operator has been selected for the conjunction operator and the t-norm from the compositional. Figures 6 and 7 display the gaussian membership function of input and output linguistic variables.

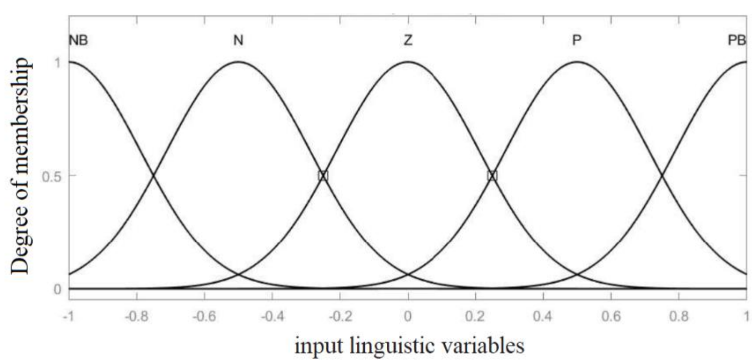

Figure 6: Membership functions of input linguistic variables $s_t, \dot{s}_t, s_d, and\ \dot{s}_d$.

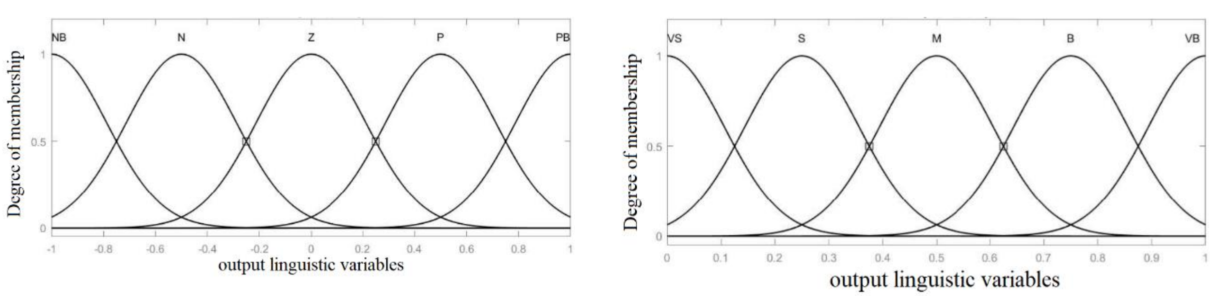

(a) (b)

Figure 7: Membership functions of (a) output linguistic variables F_{st} and F_{sd} (b) output linguistic variables K and k_d.

The membership functions for variables $F_{st}, F_{sd}\dot{s}_t$, s_t, s_d and $\dot{s}_d$ have been considered as five fuzzy partitions in which the following symbols have been used: NB (Negative Big), N (Negative), Z (Zero), P (Positive), and PB (Positive Big) and the fuzzy set is normalized in the interval (-1,1). Also, for positive variables , K and k_d the membership functions have been introduced as VS (very small), S (small) and M (medium); B (big) and VB (very big) and the fuzzy set is normalized in the interval (0,1). Tables 1 and 2 introduce the fuzzy rules base which have been implemented in the present study.

Table 1: Fuzzy rule base for F_{st} and F_{sd}.

		$\dot{s}_t$ **or** $\dot{s}_d$				
	F_{st} **or** F_{sd}	NB	N	Z	P	PB
s_t **or** s_d	NB	NB	NB	N	NB	NB
	N	NB	N	N	N	NB
	Z	N	N	Z	P	P
	P	PB	P	P	P	PB
	PB	PB	PB	P	PB	PB

Table 2: Fuzzy rule base for K or k_d.

		$\dot{s}_t$ **or** $\dot{s}_d$				
	K or k_d	NB	N	Z	P	PB
s_t **or** s_d	NB	VB	VB	B	VB	VB
	N	B	B	M	B	B
	Z	M	M	M	M	M
	P	B	B	M	B	B
	PB	VB	VB	B	VB	PB

F_{st}, F_{sd}, K and k_d are the outputs of the fuzzy logic controller, which are determined by the mapping of input linguistic variables $\dot{s}_t$, s_t, s_d and $\dot{s}_d$. The procedure of disturbance-observer-based ITSMC with fuzzy gain tuning is illustrated in Fig. 8. The fuzzy gain tuning and fast disturbance observe have been combined with ITSMC to improve the performance of the control scheme in the presence of dynamic uncertainty, external disturbance and input saturation. The rest of this paper, we will apply the proposed control scheme to the hyperchaotic finance system.

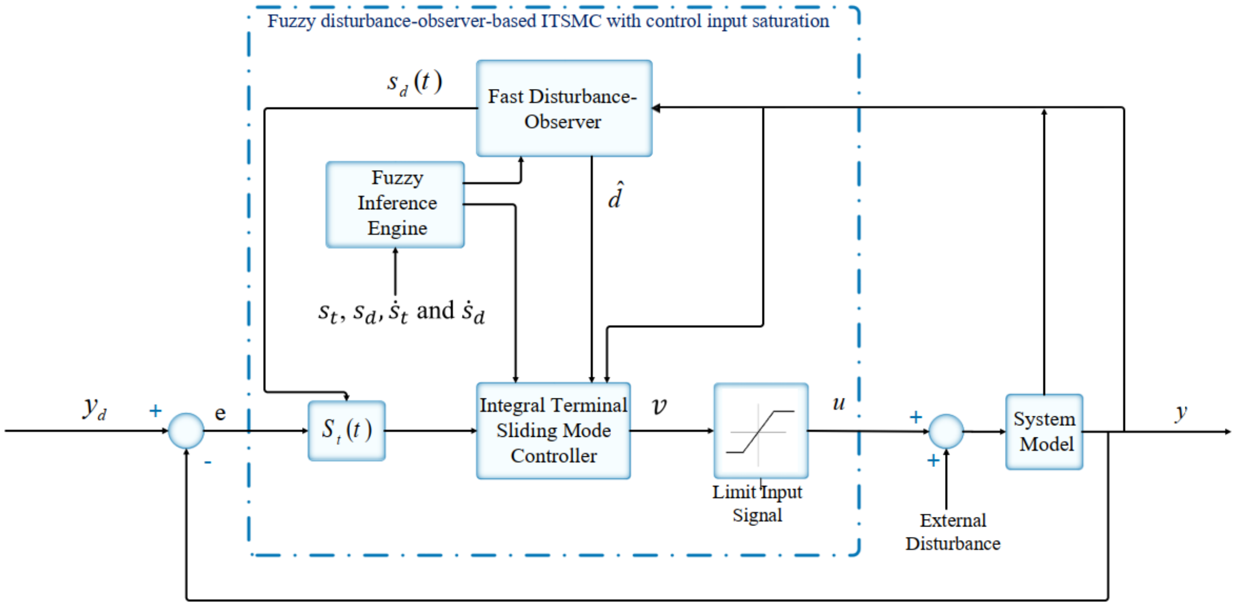

Figure 8: Scheme of fuzzy disturbance-observer-based ITSMC for MHS.

5. Simulation results

In the following section, the simulation results of the proposed fuzzy disturbance-observer-based ITSMC which is performed on the hyperchaotic finance system have been presented. The state equations of the system with external disturbance and the control input is

$$\begin{aligned}
\dot{x} &= z + (y - a)x + u + d_x + u_{cx} \\
\dot{y} &= 1 - by - x^2 + d_y + u_{cy} \\
\dot{z} &= -x - cz + d_z + u_{cz} \\
\dot{u} &= -dxy - ku + d_u + u_{cu}
\end{aligned} \tag{37}$$

According to the proposed control technique, the control input with input saturation and estimated disturbance are as follow

$$u_c = \begin{cases} u_{max} & if\ v > u_{max} \\ v & \\ u_{min} & if\ v < u_{min} \end{cases} \tag{38-a}$$

$$v = g^{-1}(X)\left(\dot{X}_d - f(X) - \left(K + \delta \left\| e^{\frac{q}{p}}(t) \right\| I\right)\ F_{st} - \widehat{D}_X\right) \tag{38-b}$$

$$\hat{d} = -ks_d - \beta sign(s_d) - \varepsilon {s_d}^{p_0/q_0} - |f(X)|\ F_{sd} - f(X) \tag{38-c}$$

Where vectors $u_c = \left[u_{cx}, u_{cy}\ , u_{cz}, u_{cw}\right]$, $X = [x, y, z, u]$ and $D = \left[D_x, D_y\ , D_z, D_u\right]$ are the limited control input, the state of the system and external disturbance, respectively.

5.1 Comparison of the proposed control scheme with SMC

To investigate the advantages of the developed control scheme, the proposed controller is compared with the SMC based on the disturbance observer which developed by Chen and Chen [36]. The initial conditions are considered as $[0.1, 0.2, 0.6, -0.3]$. Also, the control signals are turned on at $T_{start} = 1.$ The designed parameters for the control scheme are considered as

$$\begin{aligned} &p_0 = p = [3,3,3,3], q = [13,13,13,13,13], q_0 = [9,9,9,9], \delta = [5,5,5,5] \\ &\beta = [100,100,100,100], \varepsilon = [10,10,10,10] \end{aligned} \tag{39}$$

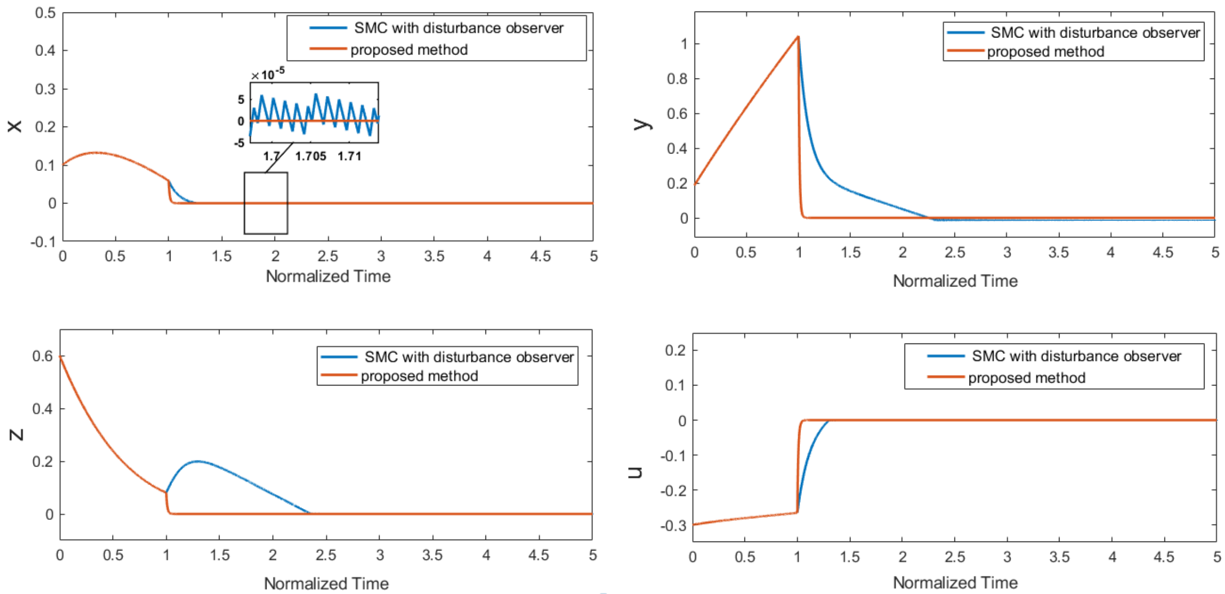

Figure 9: Time history of the hyperchaotic financial systems with the fuzzy disturbance-observer-based ITSMC and disturbance-observer-based sliding mode control. The control signals are turned on at $T_{start} = 1$.

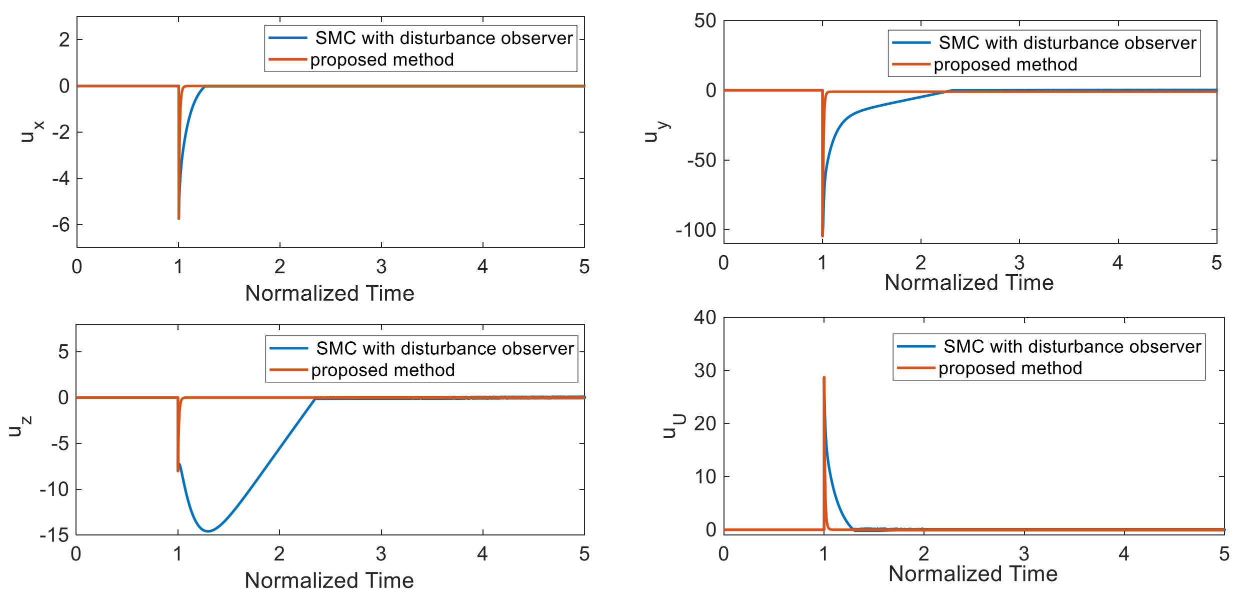

Figure 10: The control input of the hyperchaotic financial systems with the fuzzy disturbance-observer-based ITSMC and disturbance-observer-based sliding mode control ($T_{start} = 1$).

Figures 9 and 10 illustrate the time history of the system and control input by using both the control method. It is concluded from Figure 9 that the proposed fuzzy disturbance-observer based ITSMC presents an accurate and very faster response over the disturbance-observer based SMC method. Also, the system with fuzzy disturbance-observer based ITSMC has the smooth and chattering-free sliding surfaces, due to the proposed fuzzy inference engine. Therefore, the suggested control scheme has fine performance in comparison with the conventional SMC [36].

As is shown in Figure 10 large input control is needed for both control schemes. In the practical systems, an appropriate control input saturation should be considered to avoid large input. To address this problem, we consider the feasible input saturation as follow

$$u_{c_{max}} = [5,5,5,5] \qquad u_{c_{min}} = [-5,-5,-5,-5] \tag{40}$$

moreover, we consider the system in the presence of external disturbances as follow

$$d_{\mathrm{x}} = d_{\mathrm{y}} = d_{\mathrm{z}} = d_{\mathrm{w}} = .1\sin(10t) + .1\cos(5t) \tag{41}$$

Figures 11 and 12 show the time history of states and control input by applying fuzzy disturbance-observer-based ITSMC in the presence of input saturation and external disturbance. Also, Figure 13 displays estimated disturbance by disturbance observer.

The results of the suggested control technique and SMC are summarized in Tables 3, 4, and 5. Table 3 lists the values of the rise time (T_r) and settling time (T_s) for states of the system. Also, Table 4 presents the values of the regulation errors of the system. From these results, it can be concluded that the closed-loop convergence times of the system with SMC is more than the proposed controller. Table 5 compares the control input value for the SMC and the proposed controller. According to this table, the control input norms of the proposed method with input saturation are less than SMC, which is because of input saturation and free chattering response due to the fuzzy logic inference engine. This yields less energy consumption for the control of the finance system. Since the value of the control input is important for the financial purpose, control input saturation plays an inevitable role for these systems.

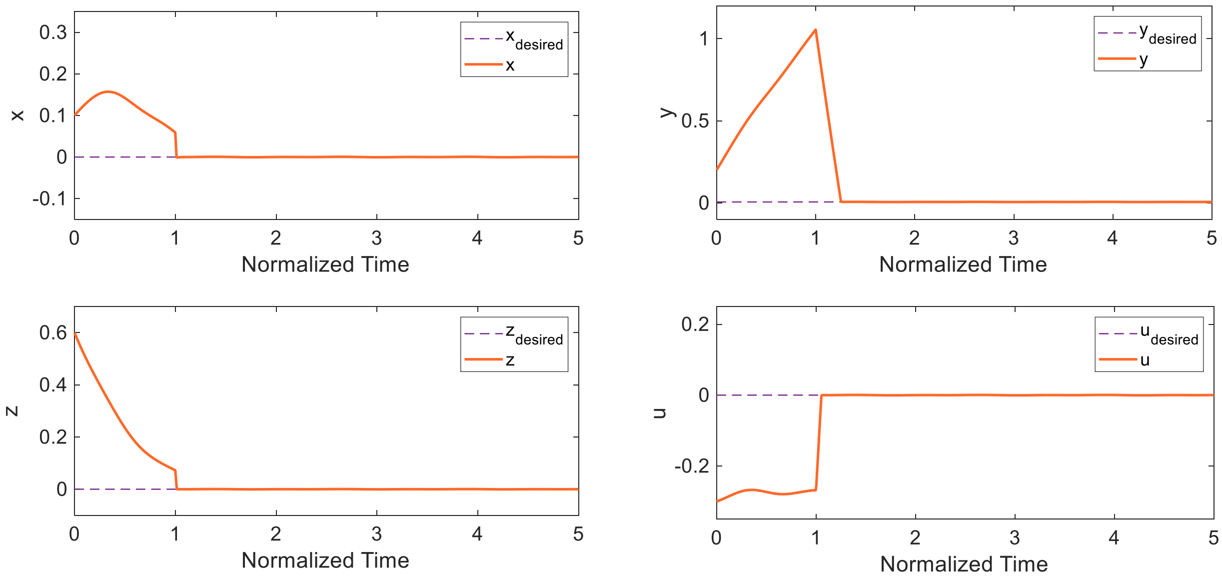

Figure 11: Time history of the hyperchaotic financial systems with the fuzzy disturbance-observer-based ITSMC in the presence of input saturation and external disturbance ($T_{start} = 1$).

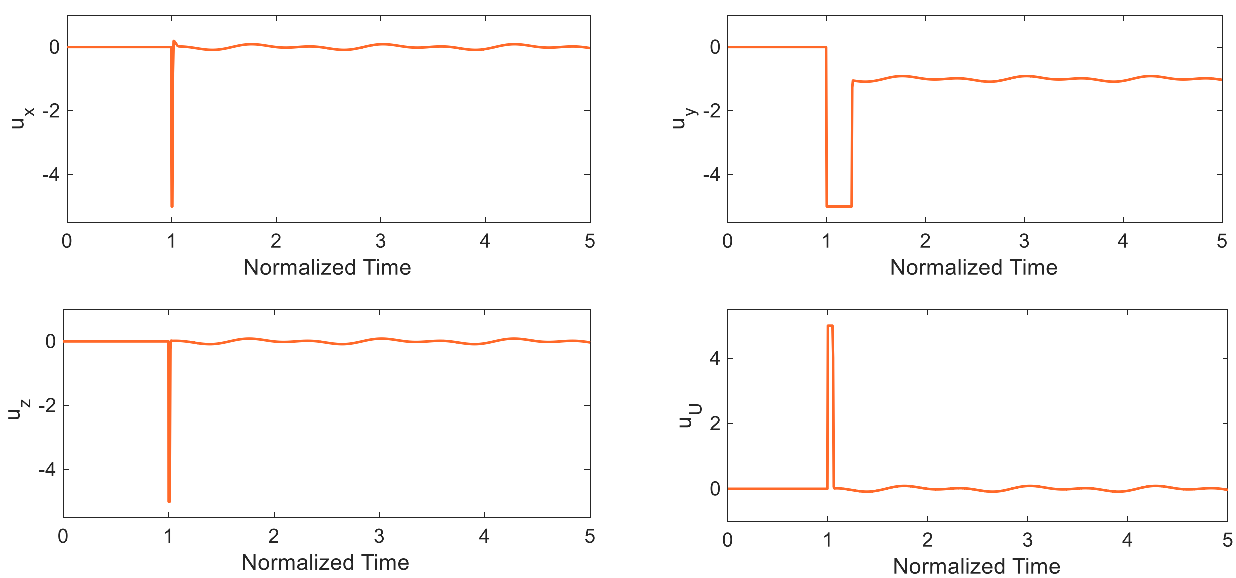

Figure 12: The control input of the hyperchaotic financial systems with the fuzzy disturbance-observer-based ITSMC in the presence of input saturation and external disturbance ($T_{start} = 1$).

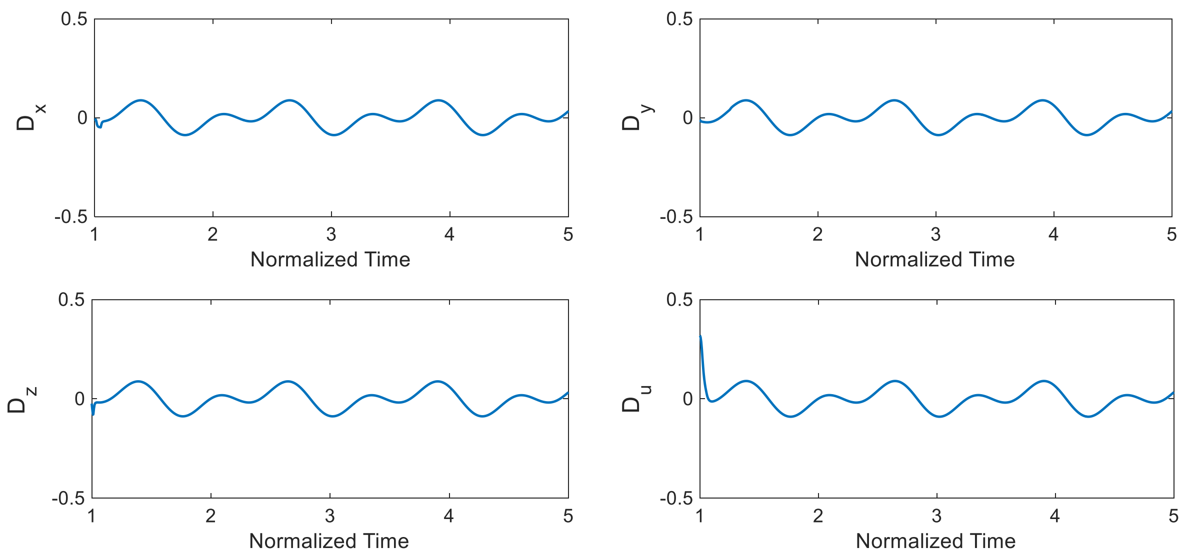

Figure 13: The disturbances estimated with fuzzy disturbance-observer ($T_{start} = 1$).

Table 3: Quantitative comparison of the settling time (T_s) and the rise time (T_r)

	$\boldsymbol{T_r(x)}$	$\boldsymbol{T_s(x)}$	$\boldsymbol{T_r(y)}$	$\boldsymbol{T_s(y)}$	$\boldsymbol{T_r(z)}$	$\boldsymbol{T_s(z)}$	$\boldsymbol{T_r(w)}$	$\boldsymbol{T_s(w)}$
Proposed method	0.2113	1.0353	0.0224	1.0382	0.9405	1.0204	0.1625	1.0417
Proposed method in the presence of input saturation and external disturbance	0.1949	1.0408	0.0389	1.2502	0.9356	1.0318	0.7754	1.0525
SMC (Chen and Chen (2013))	0.3430	1.2199	0.7675	2.2135	2.0090	2.3008	0.3597	1.2831

Table 4: Quantitative comparison of the regulation errors.

	$\|\boldsymbol{e_x}\|_2$	$\|\boldsymbol{e_x}\|_\infty$	$\|\boldsymbol{e_y}\|_2$	$\|\boldsymbol{e_y}\|_\infty$	$\|\boldsymbol{e_z}\|_2$	$\|\boldsymbol{e_z}\|_\infty$	$\|\boldsymbol{e_w}\|_2$	$\|\boldsymbol{e_w}\|_\infty$
Proposed method	0.4332	0.0589	7.5410	1.0588	0.5874	0.0806	1.8699	0.2656
Proposed method in the presence of input saturation and external disturbance	0.3736	0.0588	30.6730	1.0548	0.5097	0.0726	3.5944	0.2681
SMC (Chen and Chen (2013))	1.2506	0.0589	31.2722	1.0588	15.7564	0.1988	6.2587	0.2656

Table 5: Quantitative comparison of the control input

	$\|\boldsymbol{u}_x\|_2$	$\|\boldsymbol{u}_x\|_\infty$	$\|\boldsymbol{u}_y\|_2$	$\|\boldsymbol{u}_y\|_\infty$	$\|\boldsymbol{u}_z\|_2$	$\|\boldsymbol{u}_z\|_\infty$	$\|\boldsymbol{u}_w\|_2$	$\|\boldsymbol{u}_w\|_\infty$
Proposed method	39.2421	5.6184	802.6640	104.8196	54.7737	7.9059	191.4764	28.5568
Proposed method in the presence of input saturation and external disturbance	52.8253	5.0000	318.0940	5.0000	59.0629	5.0000	115.3672	5.0000
SMC (Chen and Chen (2013))	270.4521	5.0770	431.4070	99.4440	302.310 3	14.6431	370.0206	27.6923

5.2 synchronization of chaotic systems with uncertainties and input saturation

In this state, the efficient fuzzy disturbance-observer-based TSMC scheme is employed to achieve the synchronization of the system. The slave system is taken from Eq. (37), while the master system takes the form:

$$\begin{aligned} \dot{x} &= z_m + (y_m - a)x_m + u_m \\ \dot{y} &= 1 - by_m - x_m^2 \\ \dot{z} &= -x_m - cz_m \\ \dot{u} &= -dx_m y_m - ku_m \end{aligned} \tag{42}$$

The parameters of the master system are considered equal to the slave system. Also, the initial conditions for the master system are [0, 2, 0.1, -0.5]. We consider the case where we have poor knowledge of the slave system parameters. This way, we set parameters to 50% of their actual values, i.e

$$\hat{a} = 0.5 \times a, \hat{b} = 0.5 \times b, \ \hat{c} = 0.5 \times c, \hat{d} = 0.5 \times d, \ \hat{k} = 0.5 \times k \tag{43}$$

Where the prameters $\hat{a}, \hat{b}, \hat{c},\ \hat{d}\ and\ \hat{k}$ are incorrect parameters and have been used for control scheme instead of a, b, c, d and k. Actually, we feed the controller with these incorrect information to investigate the performance of the proposed controller in presence of uncertainity. The time-history of synchronization and control input are illustrated in Figures 14 and 15, respectively. Based on these figures, the proposed control scheme swiftly moves the slave system response to the master system response.

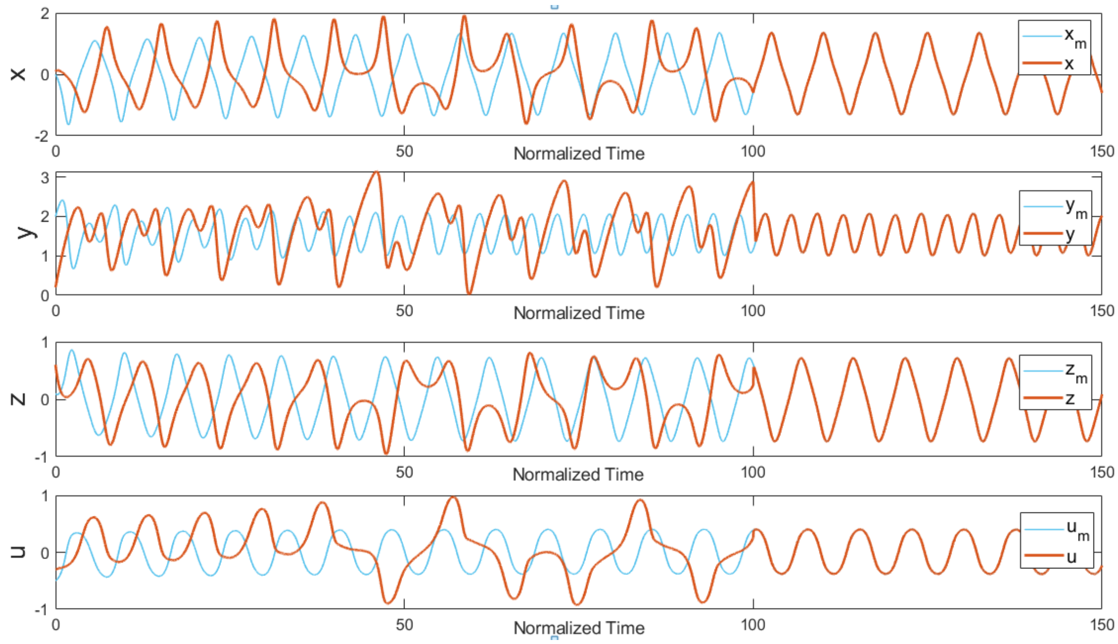

Figure 14: Synchronization results for the hyperchaotic financial systems with the fuzzy disturbance-observer-based ITSMC which the control signals are turned on at $T_{start} = 100$. The slave and master system are color coded orange and blue, respectively.

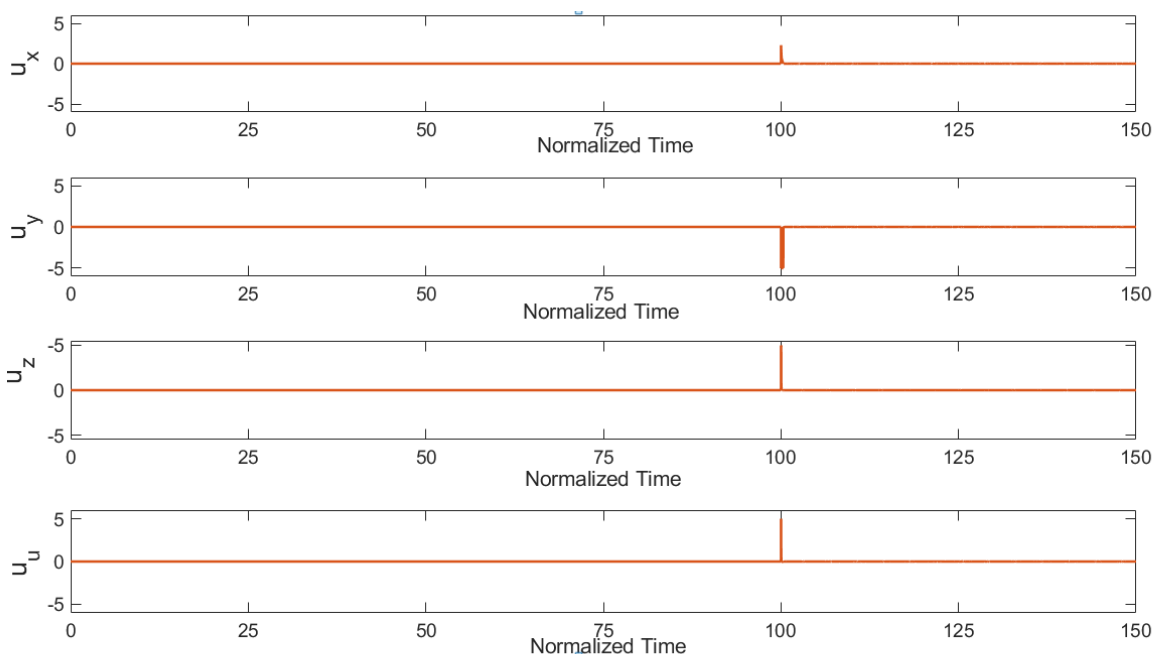

Figure 15: The control input for Synchronization of the hyperchaotic financial systems with the fuzzy disturbance-observer-based ITSMC which the control signals are turned on at $T_{start} = 100$.

Simulation results show that the proposed fuzzy disturbance-observer-based ITSMC successfully moves the system to the desired value in presence of external disturbances and control input saturation, even when knowledge of the system parameters is incorrect. Thereupon, the proposed control technique could be applied to a wide range of nonlinear systems to ensure that they are always operating in the desired mode.

Conclusion

This paper has presented a four-dimensional hyperchaotic finance system with specific features. Its dynamic behaviour has been thoroughly featured through bifurcation diagrams, phase portraits, Lyapunov exponents diagrams, and entropy-based analyses. A novel robust fuzzy disturbance-observer based integral terminal sliding mode control algorithm has also been designed to control and synchronize the system. The output of this fast disturbance-observer has been used to develop integral terminal sliding mode control in presence of uncertainties, external disturbances and control input saturation. Additionally, the designed controller has been adapted by implementing the fuzzy rules. Based on the presented simulation results, it can be concluded that the proposed control scheme is appropriate to control the financial hyperchaotic system. As a future suggestion, the proposed control scheme could be developed for higher relative degree systems. Moreover, this study could also be extended for non-integer order financial systems.

References

[1] Rossler OE. An equation for hyperchaos. Physics Letters A. 1979;71:155-7.
[2] Rong CG, Xiaoning D. From chaos to order: methodologies, perspectives and applications: World Scientific; 1998.
[3] Chen A, Lu J, Lü J, Yu S. Generating hyperchaotic Lü attractor via state feedback control. Physica A: Statistical Mechanics and its Applications. 2006;364:103-10.

[4] Nikolov S, Clodong S. Occurrence of regular, chaotic and hyperchaotic behavior in a family of modified Rossler hyperchaotic systems. Chaos, Solitons & Fractals. 2004;22:407-31.
[5] Ma C, Wang X. Hopf bifurcation and topological horseshoe of a novel finance chaotic system. Communications in Nonlinear Science and Numerical Simulation. 2012;17:721-30.
[6] Gao Q, Ma J. Chaos and Hopf bifurcation of a finance system. Nonlinear Dynamics. 2009;58:209.
[7] David SA, Machado JAT, Quintino DD, Balthazar JM. Partial chaos suppression in a fractional order macroeconomic model. Mathematics and Computers in Simulation. 2016;122:55-68.
[8] Hołyst JA, Urbanowicz K. Chaos control in economical model by time-delayed feedback method. Physica A: Statistical Mechanics and its Applications. 2000;287:587-98.
[9] Iwaszczuk N, Kavalets I. Delayed feedback control method for generalized Cournot-Puu oligopoly model/in "Selected Economic and Technological Aspects of Management", ed. N Iwaszczuk, Krakow. 2013:108-23.
[10] Hajipour M, Jajarmi A, Baleanu D. An efficient nonstandard finite difference scheme for a class of fractional chaotic systems. Journal of Computational and Nonlinear Dynamics. 2018;13:021013.
[11] Yu H, Cai G, Li Y. Dynamic analysis and control of a new hyperchaotic finance system. Nonlinear Dynamics. 2012;67:2171-82.
[12] Tirandaz H, Aminabadi SS, Tavakoli H. Chaos synchronization and parameter identification of a finance chaotic system with unknown parameters, a linear feedback controller. Alexandria engineering journal. 2018;57:1519-24.
[13] Fuh C-C, Tsai H-H, Yao W-H. Combining a feedback linearization controller with a disturbance observer to control a chaotic system under external excitation. Communications in Nonlinear Science and Numerical Simulation. 2012;17:1423-9.
[14] Yu J, Lei J, Wang L. Backstepping synchronization of chaotic system based on equivalent transfer function method. Optik. 2017;130:900-13.
[15] Shukla MK, Sharma BB. Stabilization of a class of fractional order chaotic systems via backstepping approach. Chaos, Solitons & Fractals. 2017;98:56-62.
[16] Mahmoodabadi MJ, Jahanshahi H. Multi-objective optimized fuzzy-PID controllers for fourth order nonlinear systems. Engineering Science and Technology, an International Journal. 2016;19:1084-98.
[17] Jahanshahi H, Jafarzadeh M, Sari NN, Pham V-T, Huynh VV, Nguyen XQ. Robot Motion Planning in an Unknown Environment with Danger Space. Electronics. 2019;8:201.
[18] Jahanshahi H, Rajagopal K, Akgul A, Sari NN, Namazi H, Jafari S. Complete analysis and engineering applications of a megastable nonlinear oscillator. International Journal of Non-Linear Mechanics. 2018;107:126-36.
[19] Jahanshahi H, Shahriari-Kahkeshi M, Alcaraz R, Wang X, Singh VP, Pham V-T. Entropy Analysis and Neural Network-based Adaptive Control of a Non-Equilibrium Four-Dimensional Chaotic System with Hidden Attractors. Entropy. 2019;21:156.
[20] Tsai JS-H, Fang J-S, Yan J-J, Dai M-C, Guo S-M, Shieh L-S. Hybrid robust discrete sliding mode control for generalized continuous chaotic systems subject to external disturbances. Nonlinear Analysis: Hybrid Systems. 2018;29:74-84.
[21] Jahanshahi H. Smooth control of HIV/AIDS infection using a robust adaptive scheme with decoupled sliding mode supervision. The European Physical Journal Special Topics. 2018;227:707-18.
[22] Yao HX, Wu CY, Jiang DP, Ding J. Chaos control in an investment model with straight-line stabilization method. Nonlinear Analysis: Real World Applications. 2008;9:651-62.
[23] Vargas JAR, Grzeidak E, Hemerly EM. Robust adaptive synchronization of a hyperchaotic finance system. Nonlinear Dynamics. 2015;80:239-48.
[24] Jajarmi A, Hajipour M, Baleanu D. New aspects of the adaptive synchronization and hyperchaos suppression of a financial model. Chaos, Solitons & Fractals. 2017;99:285-96.

[25] Dadras S, Momeni HR. Control of a fractional-order economical system via sliding mode. Physica A: Statistical Mechanics and its Applications. 2010;389:2434-42.
[26] Wang Z, Huang X, Shen H. Control of an uncertain fractional order economic system via adaptive sliding mode. Neurocomputing. 2012;83:83-8.
[27] Azar AT, Zhu Q. Advances and applications in sliding mode control systems: Springer; 2015.
[28] González JA, Barreiro A, Dormido S, Baños A. Nonlinear adaptive sliding mode control with fast non-overshooting responses and chattering avoidance. Journal of the Franklin Institute. 2017;354:2788-815.
[29] Mobayen S. Finite-time stabilization of a class of chaotic systems with matched and unmatched uncertainties: An LMI approach. Complexity. 2016;21:14-9.
[30] Laghrouche S, Plestan F, Glumineau A. Higher order sliding mode control based on integral sliding mode. Automatica. 2007;43:531-7.
[31] Rajaei A, Vahidi-Moghaddam A, Ayati M, Baghani M. Integral sliding mode control for nonlinear damped model of arch microbeams. Microsystem Technologies. 2019;25:57-68.
[32] Chihi A, Azza HB, Jemli M, Sellami A. Nonlinear integral sliding mode control design of photovoltaic pumping system: Real time implementation. ISA transactions. 2017;70:475-85.
[33] Mobayen S. Chaos synchronization of uncertain chaotic systems using composite nonlinear feedback based integral sliding mode control. ISA transactions. 2018;77:100-11.
[34] Furat M, Eker İ. Second-order integral sliding-mode control with experimental application. ISA transactions. 2014;53:1661-9.
[35] Khan A, Bhat MA. Hyper-chaotic analysis and adaptive multi-switching synchronization of a novel asymmetric non-linear dynamical system. International Journal of Dynamics and Control. 2017;5:1211-21.
[36] Chen M, Chen WH. Sliding mode control for a class of uncertain nonlinear system based on disturbance observer. International Journal of Adaptive Control and Signal Processing. 2010;24:51-64.
[37] Gomez I, Losada M, Lombardi O. About the concept of quantum chaos. Entropy. 2017;19:205.
[38] Young L-S. Entropy in dynamical systems. Entropy. 2003;313.
[39] Grassberger P, Procaccia I. Estimation of the Kolmogorov entropy from a chaotic signal. Physical review A. 1983;28:2591.
[40] Richman JS, Moorman JR. Physiological time-series analysis using approximate entropy and sample entropy. American Journal of Physiology-Heart and Circulatory Physiology. 2000;278:H2039-H49.
[41] Fouda JSAE, Koepf W, Jacquir S. The ordinal Kolmogorov-Sinai entropy: A generalized approximation. Communications in Nonlinear Science and Numerical Simulation. 2017;46:103-15.
[42] Bandt C, Pompe B. Permutation entropy: a natural complexity measure for time series. Physical review letters. 2002;88:174102.
[43] Zanin M, Zunino L, Rosso OA, Papo D. Permutation entropy and its main biomedical and econophysics applications: a review. Entropy. 2012;14:1553-77.
[44] Keller K, Unakafov A, Unakafova V. Ordinal patterns, entropy, and EEG. Entropy. 2014;16:6212-39.
[45] Azami H, Escudero J. Amplitude-aware permutation entropy: Illustration in spike detection and signal segmentation. Computer methods and programs in biomedicine. 2016;128:40-51.
[46] Zhihong M, Yu XH. Terminal sliding mode control of MIMO linear systems. IEEE. p. 4619-24.
[47] Chen M, Wu Q-X, Cui R-X. Terminal sliding mode tracking control for a class of SISO uncertain nonlinear systems. ISA transactions. 2013;52:198-206.
[48] Chiu C-S. Derivative and integral terminal sliding mode control for a class of MIMO nonlinear systems. Automatica. 2012;48:316-26.